

# Relativistic effects on the back-to-back correlation functions of boson-antiboson pairs in high energy heavy ion collisions<sup>\*</sup>

 ZHANG Yong YANG Jing ZHANG Wei-Ning<sup>1)</sup>

School of Physics and Optoelectronic Technology, Dalian University of Technology, Dalian, Liaoning 116024, China

**Abstract:** We calculate the back-to-back correlation (BBC) functions of relativistic boson-antiboson pairs in high energy heavy ion collisions using the Monte Carlo method. The relativistic effects on the BBC functions of  $\phi\phi$  and  $K^+K^-$  pairs are investigated. The investigations indicate that the relativistic effects on the BBC functions of  $K^+K^-$  pairs with large momenta are significant, and the effect is sensitive to the particle freeze-out temperature.

**Key words:** back-to-back correlation boson-antiboson pair, relativistic effect, mass-shift, high energy heavy ion collision

**PACS:** 25.75.Gz, 21.65.jk

## 1 Introduction

In the hot and dense hadronic sources created in high energy heavy ion collisions, the boson mass-shift due to the medium interactions might lead to a measurable back-to-back correlation (BBC) of boson-antiboson pairs [1, 2]. This medium-effective BBC is different from the pure Bose-Einstein statistic correlations between the bosons with different isospin [3], which are negligible as compared to the BBC in high energy heavy ion collisions [2, 4]. Denote  $a_{\mathbf{k}}(a_{\mathbf{k}}^\dagger)$  as the annihilation (creation) operators of the freeze-out boson with momentum  $\mathbf{k}$  and mass  $m$ , and  $b_{\mathbf{k}}(b_{\mathbf{k}}^\dagger)$  as the annihilation (creation) operators of the corresponding quasiparticle with momentum  $\mathbf{k}$  and shifted mass  $m_*$  in the homogenous medium. They are related by the Bogoliubov transformation [1, 2]

$$a_{\mathbf{k}} = c_{\mathbf{k}} b_{\mathbf{k}} + s_{-\mathbf{k}}^* b_{-\mathbf{k}}^\dagger, \quad (1)$$

where

$$c_{\mathbf{k}} = \cosh f_{\mathbf{k}}, \quad s_{\mathbf{k}} = \sinh f_{\mathbf{k}}, \quad f_{\mathbf{k}} = \frac{1}{2} \log(\omega_{\mathbf{k}}/\Omega_{\mathbf{k}}), \quad (2)$$

$$\omega_{\mathbf{k}} = \sqrt{\mathbf{k}^2 + m^2}, \quad \Omega_{\mathbf{k}} = \sqrt{\mathbf{k}^2 + m_*^2}. \quad (3)$$

The BBC function is defined as [1, 2]

$$C(\mathbf{k}, -\mathbf{k}) = 1 + \frac{|G_s(\mathbf{k}, -\mathbf{k})|^2}{G_c(\mathbf{k}, \mathbf{k})G_c(-\mathbf{k}, -\mathbf{k})}, \quad (4)$$

where  $G_c(\mathbf{k}_1, \mathbf{k}_2)$  and  $G_s(\mathbf{k}_1, \mathbf{k}_2)$  are the chaotic and squeezed amplitudes, respectively, as

$$G_c(\mathbf{k}_1, \mathbf{k}_2) = \sqrt{\omega_{\mathbf{k}_1}\omega_{\mathbf{k}_2}} \langle a_{\mathbf{k}_1}^\dagger a_{\mathbf{k}_2} \rangle, \quad (5)$$

$$G_s(\mathbf{k}_1, \mathbf{k}_2) = \sqrt{\omega_{\mathbf{k}_1}\omega_{\mathbf{k}_2}} \langle a_{\mathbf{k}_1} a_{\mathbf{k}_2} \rangle, \quad (6)$$

where  $\langle \dots \rangle$  means ensemble average.

In Refs. [5–7], S. Padula *et al.* studied the BBC functions of  $\phi\phi$  and  $K^+K^-$  based on the non-relativistic formalism [5] for local-equilibrium expanding sources in high energy heavy ion collisions. In this work we investigate the BBC functions of  $\phi\phi$  and  $K^+K^-$  for the local-equilibrium expanding sources in a relativistic case, using Monte Carlo calculations. Our results indicate that the relativistic effects on the BBC functions of  $K^+K^-$  pairs with large momenta are significant, and the effect is sensitive to the particle freeze-out temperature.

## 2 BBC function for local-equilibrium expanding source

### 2.1 The formulas of BBC function

For local-equilibrium expanding sources,  $G_c(\mathbf{k}_1, \mathbf{k}_2)$  and  $G_s(\mathbf{k}_1, \mathbf{k}_2)$  can be expressed as [2, 8]

$$G_c(\mathbf{k}_1, \mathbf{k}_2) = \int \frac{d^4\sigma_\mu(x)}{(2\pi)^3} K_{1,2}^\mu e^{iq_{1,2}\cdot x} \left\{ |c'_{\mathbf{k}'_1, \mathbf{k}'_2}|^2 n'_{\mathbf{k}'_1, \mathbf{k}'_2} + |s'_{-\mathbf{k}'_1, -\mathbf{k}'_2}|^2 [n'_{-\mathbf{k}'_1, -\mathbf{k}'_2} + 1] \right\}, \quad (7)$$

$$G_s(\mathbf{k}_1, \mathbf{k}_2) = \int \frac{d^4\sigma_\mu(x)}{(2\pi)^3} K_{1,2}^\mu e^{2iq_{1,2}\cdot x} \left\{ s'^*_{-\mathbf{k}'_1, \mathbf{k}'_2} c'_{\mathbf{k}'_2, -\mathbf{k}'_1} \times n'_{-\mathbf{k}'_1, \mathbf{k}'_2} + c'_{\mathbf{k}'_1, -\mathbf{k}'_2} s'^*_{-\mathbf{k}'_2, \mathbf{k}'_1} [n'_{\mathbf{k}'_1, -\mathbf{k}'_2} + 1] \right\}. \quad (8)$$

Here,  $d^4\sigma^\mu(x) = d^3\Sigma^\mu(x; \tau_f) F(\tau_f) d\tau_f$ ,  $d^3\Sigma^\mu(x; \tau_f)$  is the normal-oriented volume element depending on the freeze-out hypersurface parameter  $\tau_f$ ,  $F(\tau_f)$  is the invariant distribution of the local time parameter,  $q_{1,2}^\mu = k_1^\mu - k_2^\mu$ ,  $K_{1,2}^\mu = (k_1^\mu + k_2^\mu)/2$ , and  $\mathbf{k}'_i$  is the local-frame momentum

corresponding to  $\mathbf{k}_i$  ( $i = 1, 2$ ). The other local variables are:

$$c'_{\pm\mathbf{k}'_1, \pm\mathbf{k}'_2} = \cosh[f'_{\pm\mathbf{k}'_1, \pm\mathbf{k}'_2}], \quad (9)$$

$$s'_{\pm\mathbf{k}'_1, \pm\mathbf{k}'_2} = \sinh[f'_{\pm\mathbf{k}'_1, \pm\mathbf{k}'_2}], \quad (10)$$

$$\begin{aligned} f'_{\pm\mathbf{k}'_1, \pm\mathbf{k}'_2} &= \frac{1}{2} \log \left[ (\omega'_{\mathbf{k}'_1} + \omega'_{\mathbf{k}'_2}) / (\Omega'_{\mathbf{k}'_1} + \Omega'_{\mathbf{k}'_2}) \right] \\ &= \frac{1}{2} \log \left[ K_{1,2}^\mu u_\mu(x) / K_{1,2}^{*\nu} u_\nu(x) \right] \\ &\equiv f_{\mathbf{k}_1, \mathbf{k}_2}(x), \end{aligned} \quad (11)$$

$$\begin{aligned} \omega'_{\mathbf{k}'_i}(x) &= \sqrt{\mathbf{k}'_i{}^2(x) + m^2} = k_i^\mu u_\mu(x) \\ &= \gamma_v [\omega_{\mathbf{k}_i} - \mathbf{k}_i \cdot \mathbf{v}(x)], \end{aligned} \quad (12)$$

$$\begin{aligned} \Omega'_{\mathbf{k}'_i}(x) &= \sqrt{\mathbf{k}'_i{}^2(x) + m_*^2} \\ &= \sqrt{[k_i^\mu u_\mu(x)]^2 - m^2 + m_*^2} \\ &= k_i^{*\mu} u_\mu(x), \end{aligned} \quad (13)$$

$$\begin{aligned} n'_{\pm\mathbf{k}'_1, \pm\mathbf{k}'_2} &= \exp \left\{ - \left[ \frac{1}{2} (\Omega'_{\mathbf{k}'_1} + \Omega'_{\mathbf{k}'_2}) - \mu_{1,2}(x) \right] / T(x) \right\} \\ &= \exp \left\{ - [K_{1,2}^{*\mu} u_\mu(x) - \mu_{1,2}(x)] / T(x) \right\} \\ &\equiv n_{\mathbf{k}_1, \mathbf{k}_2}(x), \end{aligned} \quad (14)$$

where,  $K_{1,2}^{*\mu} = (k_1^{*\mu} + k_2^{*\mu})/2$ ,  $u^\mu(x) = \gamma_v [1, \mathbf{v}(x)]$  is source velocity,  $\mu_{1,2}(x)$  is pair chemical potential, and  $T(x)$  is source temperature, respectively. Eq. (13) gives the relationship between  $k^{*\mu} u_\mu(x)$  and  $k^\mu u_\mu(x)$ , which will be used in calculating  $f_{\mathbf{k}_1, \mathbf{k}_2}(x)$  and  $n_{\mathbf{k}_1, \mathbf{k}_2}(x)$  for the expanding sources.

We take the source distribution in our calculations as

$$\rho(\mathbf{r}) = C e^{-r^2/(2R^2)} \theta(r - 2R), \quad (15)$$

where  $C$  is the normalization constant, and  $R$  is the source radius. The source velocity is taken as

$$\mathbf{v}(x) = \langle u \rangle \mathbf{r} / (2R), \quad (16)$$

where  $\langle u \rangle$  is a velocity parameter [5]. The emission time distribution is taken to be the typical exponential decay [2, 5–7],

$$F(\tau) = \frac{\theta(\tau - \tau_0)}{\Delta t} e^{-(\tau - \tau_0)/\Delta t}, \quad (17)$$

where  $\Delta t$  is a free parameter, and the effect of  $F(\tau)$  on the BBC function (4) is to multiply the second term by the factor  $|\tilde{F}(\omega_{\mathbf{k}} + \omega_{-\mathbf{k}}, \Delta t)|^2 = [1 + (\omega_{\mathbf{k}} + \omega_{-\mathbf{k}})^2 \Delta t^2]^{-1}$  [2, 5–7]. In the calculations of the BBC functions of boson-antiboson pairs, we take  $\mu_{1,2} = 0$ , and the parameters  $R$  and  $\Delta t$  are taken to be 7 fm and 2 fm/c [5–7].

For the considered source and with the sudden freeze-out assumption [2, 5–7], we have

$$\begin{aligned} G_c(\mathbf{k}_1, \mathbf{k}_2) &= \frac{K_{1,2}^0 \tilde{F}(\omega_{\mathbf{k}_1} - \omega_{\mathbf{k}_2}, \Delta t)}{(2\pi)^3} \int d^3 r e^{i(\mathbf{k}_1 - \mathbf{k}_2) \cdot \mathbf{r}} \\ &\times e^{-r^2/2R^2} \left\{ |c_{\mathbf{k}_1, \mathbf{k}_2}(x)|^2 n_{\mathbf{k}_1, \mathbf{k}_2}(x) \right. \\ &\left. + |s_{\mathbf{k}_1, \mathbf{k}_2}(x)|^2 [n_{\mathbf{k}_1, \mathbf{k}_2}(x) + 1] \right\}, \end{aligned} \quad (18)$$

$$\begin{aligned} G_s(\mathbf{k}_1, \mathbf{k}_2) &= \frac{K_{1,2}^0 \tilde{F}(\omega_{\mathbf{k}_1} + \omega_{\mathbf{k}_2}, \Delta t)}{(2\pi)^3} \int d^3 r e^{i(\mathbf{k}_1 + \mathbf{k}_2) \cdot \mathbf{r}} \\ &\times e^{-r^2/2R^2} \left\{ s_{\mathbf{k}_1, \mathbf{k}_2}^*(x) c_{\mathbf{k}_2, \mathbf{k}_1}(x) n_{\mathbf{k}_1, \mathbf{k}_2}(x) \right. \\ &\left. + c_{\mathbf{k}_1, \mathbf{k}_2}(x) s_{\mathbf{k}_2, \mathbf{k}_1}^*(x) [n_{\mathbf{k}_1, \mathbf{k}_2}(x) + 1] \right\}, \end{aligned} \quad (19)$$

where

$$c_{\mathbf{k}_1, \mathbf{k}_2}(x) = \cosh[f_{\mathbf{k}_1, \mathbf{k}_2}(x)] = c'_{\pm\mathbf{k}'_1, \pm\mathbf{k}'_2}, \quad (20)$$

$$s_{\mathbf{k}_1, \mathbf{k}_2}(x) = \sinh[f_{\mathbf{k}_1, \mathbf{k}_2}(x)] = s'_{\pm\mathbf{k}'_1, \pm\mathbf{k}'_2}, \quad (21)$$

and

$$\begin{aligned} C(\mathbf{k}, -\mathbf{k}) &= 1 + (1 + 4\omega_{\mathbf{k}}^2 \Delta t^2)^{-1} \left| \int d^3 r e^{\frac{-r^2}{2R^2}} \right. \\ &\times \left[ s_{\mathbf{k}, -\mathbf{k}}^*(x) c_{-\mathbf{k}, \mathbf{k}}(x) n_{\mathbf{k}, -\mathbf{k}}(x) \right. \\ &\left. + c_{-\mathbf{k}, \mathbf{k}}(x) s_{\mathbf{k}, -\mathbf{k}}^*(x) (n_{-\mathbf{k}, \mathbf{k}}(x) + 1) \right] \Bigg|^2 \\ &\left/ \int d^3 r e^{\frac{-r^2}{2R^2}} \left[ |c_{\mathbf{k}, \mathbf{k}}(x)|^2 n_{\mathbf{k}, \mathbf{k}}(x) \right. \right. \\ &\left. + |s_{\mathbf{k}, \mathbf{k}}(x)|^2 (n_{\mathbf{k}, \mathbf{k}}(x) + 1) \right] \\ &\left/ \int d^3 r e^{\frac{-r^2}{2R^2}} \left[ |c_{-\mathbf{k}, -\mathbf{k}}(x)|^2 n_{-\mathbf{k}, -\mathbf{k}}(x) \right. \right. \\ &\left. + |s_{-\mathbf{k}, -\mathbf{k}}(x)|^2 (n_{-\mathbf{k}, -\mathbf{k}}(x) + 1) \right]. \end{aligned} \quad (22)$$

## 2.2 Relativistic and non-relativistic results

In this subsection we present the BBC functions of  $\phi\phi$  and  $K^+K^-$  calculated by the Monte Carlo method. In the calculations of the integrations in Eq. (22), for a given  $\mathbf{k}$  we generate the magnitude of  $\mathbf{r}$  according to Eq. (15) and choose its angle with respect to  $\mathbf{k}$  in random. Then, we calculate the integrands and sum them in the  $|\mathbf{k}|$  bin. For the non-relativistic case, we use the approximation,

$$\begin{aligned} k^\mu u_\mu &= \gamma_v [\omega_{\mathbf{k}} - \mathbf{k} \cdot \langle u \rangle / (2R)] \\ &\approx \left( 1 + \frac{\mathbf{v}^2}{2} \right) \left[ m + \frac{\mathbf{k}^2}{2m} - \mathbf{k} \cdot \mathbf{r} \frac{\langle u \rangle}{2R} \right] \\ &\approx \left( 1 + \frac{\langle u \rangle^2}{8R^2} \mathbf{r}^2 \right) m + \left[ \frac{\mathbf{k}^2}{2m} - \mathbf{k} \cdot \mathbf{r} \frac{\langle u \rangle}{2R} \right] \\ &= m + \frac{1}{2m} \left\{ \mathbf{k} - \mathbf{r} \frac{\langle u \rangle}{2R} m \right\}^2. \end{aligned} \quad (23)$$

We show in Fig. 1 the BBC functions of  $\phi\phi$  in non-relativistic [panels (a) and (c)] and relativistic [panels (b) and (d)] cases for the fixed freeze-out temperature  $T = 140$  MeV [5] and the velocity parameter  $\langle u \rangle = 0$  and 0.5. The non-relativistic results are approximately

consistent with the results calculated by the formulism in Ref. [5] (see Fig. 2(c) and 2(d) in [5]), where slightly different non-relativistic approximations are used. One can see from Fig. 1 that the relativistic effect decreases the peaks of the BBC functions.

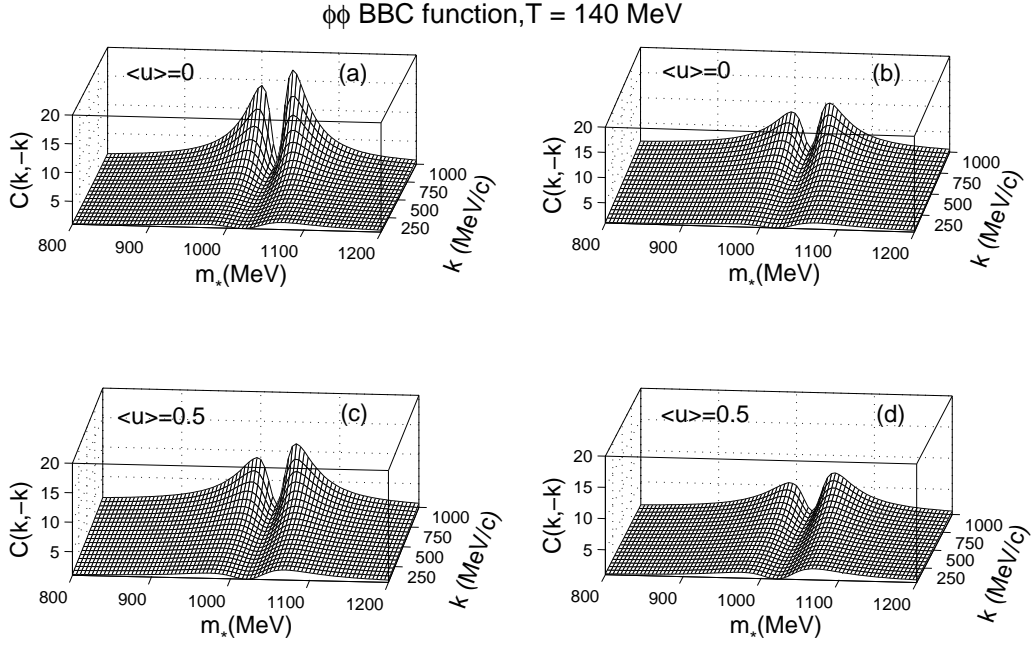


Fig. 1. The BBC functions of  $\phi\phi$  in the  $m_*$ - $k$  plane in non-relativistic [(a) and (c)] and relativistic [(b) and (d)] cases for  $T = 140$  MeV,  $\langle u \rangle = 0$  and 0.5.

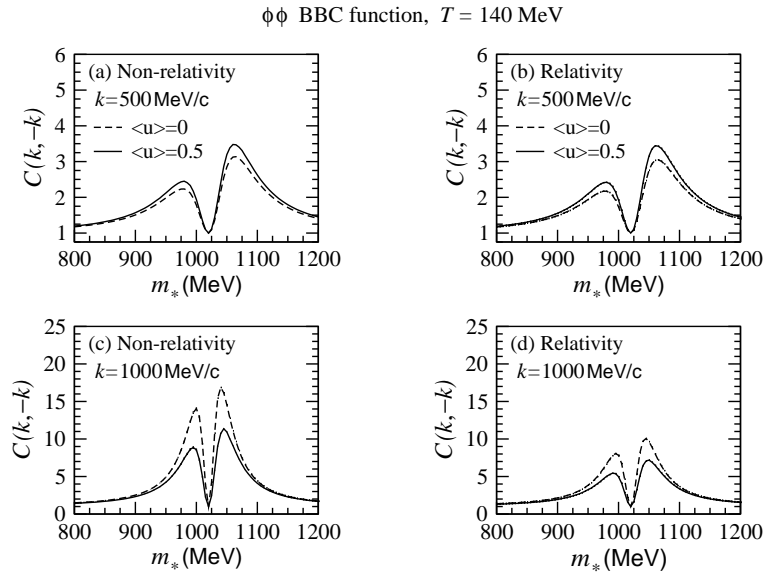


Fig. 2. The BBC functions of  $\phi\phi$  as a function of  $m_*$  at  $k = 500$  and  $1000$  MeV/c. (a) and (c) are non-relativistic results. (b) and (d) are relativistic results.

In Fig. 2 we plot the BBC functions of  $\phi\phi$  at  $k = 500$  and  $1000$  MeV/c in non-relativistic [panels (a) and (c)] and relativistic [panels (b) and (d)] cases. At  $k = 500$  MeV/c,  $k^2/m_\phi^2 \ll 1$ , the differences between the relativistic

and non-relativistic BBC functions are very small. However, at the higher  $k$ , the differences between the relativistic and non-relativistic BBC functions are larger.

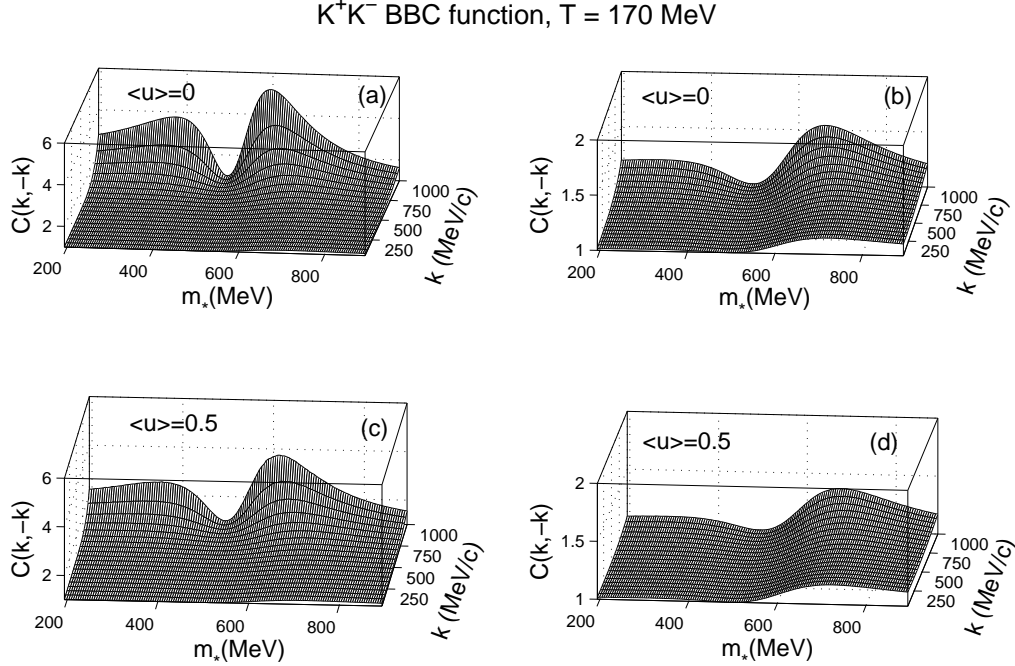


Fig. 3. The BBC functions of  $K^+K^-$  in the  $m_*-k$  plane in non-relativistic [(a) and (c)] and relativistic [(b) and (d)] cases for  $T = 170$  MeV,  $\langle u \rangle = 0$  and  $0.5$ .

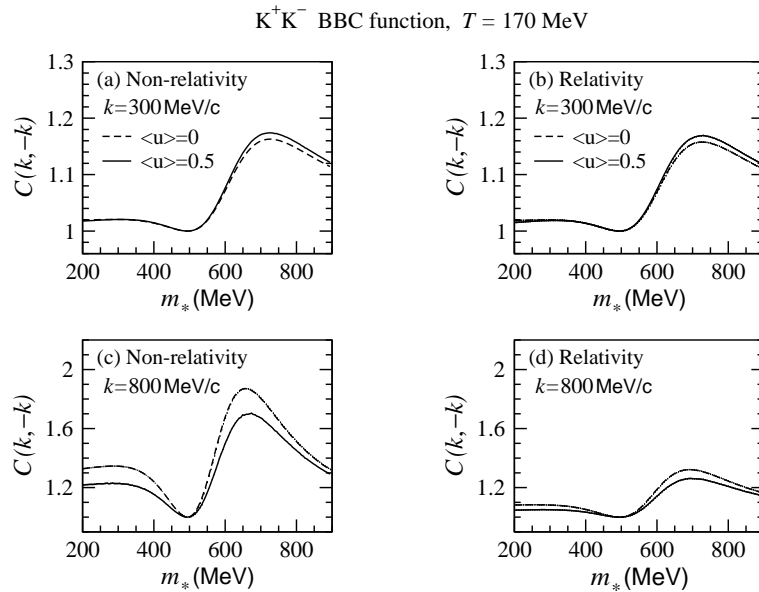


Fig. 4. The BBC functions of  $K^+K^-$  as a function of  $m_*$  at  $k = 300$  and  $800$  MeV/c. (a) and (c) are non-relativistic results. (b) and (d) are relativistic results.

In Fig. 3 we show the BBC functions of  $K^+K^-$  in non-relativistic [panels (a) and (c)] and relativistic [panels (b) and (d)] cases for the fixed freeze-out temperature  $T = 170$  MeV and the velocity parameter  $\langle u \rangle = 0$  and 0.5. It can be seen that the peaks of the relativistic BBC functions are suppressed. Further, we plot in Fig. 4 the BBC functions of  $K^+K^-$  at  $k = 300$  and  $800$  MeV/c in non-relativistic [panels (a) and (c)] and relativistic [panels (b) and (d)] cases. At the smaller  $k$ , the relativistic effect on the BBC functions is small. However, at the higher  $k$ , the relativistic effect is significant.

### 2.3 Relativistic effect on the BBC function

To examine the relativistic effect on the BBC functions of boson-antiboson pairs, we define  $D_{\text{rel}}$  as the relative difference between the relativistic and non-relativistic BBC functions  $C^{\text{Rel}}(\mathbf{k}, -\mathbf{k}) - C^{\text{Nrel}}(\mathbf{k}, -\mathbf{k})$  to  $C^{\text{Rel}}(\mathbf{k}, -\mathbf{k})$ ,

$$D_{\text{rel}} = \frac{C^{\text{Rel}}(\mathbf{k}, -\mathbf{k}) - C^{\text{Nrel}}(\mathbf{k}, -\mathbf{k})}{C^{\text{Rel}}(\mathbf{k}, -\mathbf{k})}. \quad (24)$$

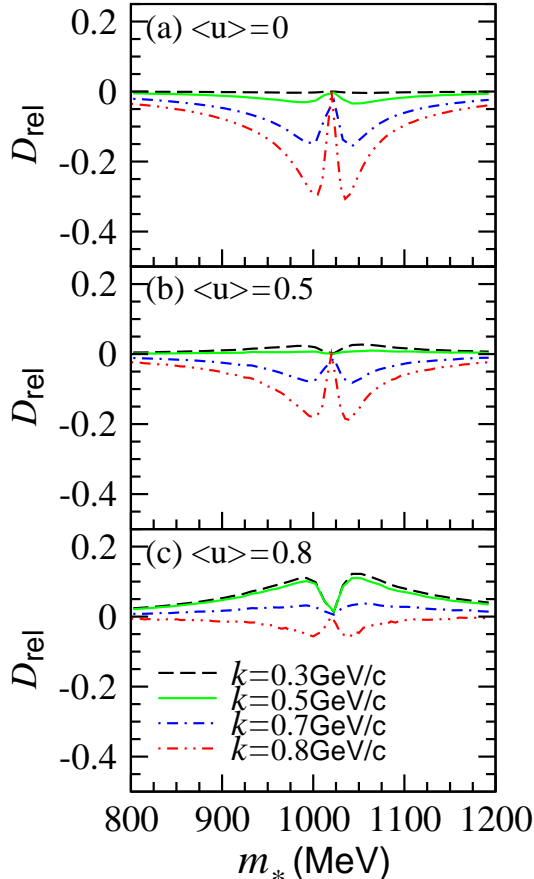


Fig. 5. The relative difference  $D_{\text{rel}}$  as a function of  $m_*$  for the  $\phi\phi$  BBC functions at  $T = 140$  MeV and with different momentum  $k$  and  $\langle u \rangle$  values.

In Fig. 5 we show the relative difference of  $\phi\phi$  relativistic and non-relativistic BBC functions at  $T = 140$  MeV. For  $\langle u \rangle = 0$ , the values of  $D_{\text{rel}}$  are negative. It means that the relativistic effect decreases the BBC function. The relativistic effect is small for low pair momentum and increases with pair momentum. At  $k = 0.8$  GeV/c, the relativistic effect may decrease the peak of BBC function by 30%. For  $\langle u \rangle = 0.5$ , the values of  $D_{\text{rel}}$  are larger than those for  $\langle u \rangle = 0$ . From Eq. (23) one can see that the nonzero  $\langle u \rangle$  equivalently reduces the momentum for the large  $\mathbf{k}$ , because Lorentz boost leads to a bigger weight for the smaller angle between  $\mathbf{k}$  and  $\mathbf{r}$ . So the difference between the relativistic and non-relativistic BBC functions decreases for the equivalent small pair momentum. However, the magnitude of the second term in the curly brace in Eq. (23) may almost be the same or even larger than  $\mathbf{k}$  magnitude for large  $\langle u \rangle$  and small  $k$ . This case leads to the positive  $D_{\text{rel}}$  results in Figs. 5(b) and 5(c).

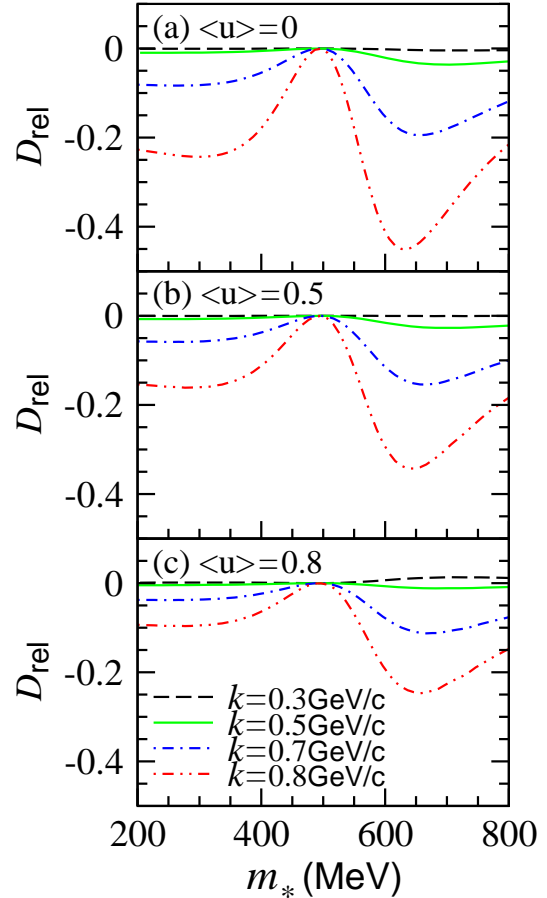


Fig. 6. The relative difference  $D_{\text{rel}}$  as a function of  $m_*$  for the  $K^+K^-$  BBC functions at  $T = 170$  MeV and with different momentum  $k$  and  $\langle u \rangle$  values.

In Fig. 6 we show the results of  $D_{\text{rel}}$  for  $K^+K^-$  relativistic and non-relativistic BBC functions at  $T =$

170 MeV. Because kaon mass is smaller than  $\phi$  mass, the difference between the  $K^+K^-$  relativistic and non-relativistic BBC functions are larger. It means the relativistic effect is important for  $K^+K^-$  BBC function. For  $k=0.8$  GeV/c and  $\langle u \rangle=0$ , one can see that the relative difference even reaches to 45%. For the largest  $\langle u \rangle$ , only the  $D_{\text{rel}}$  results for  $k=0.3$  GeV/c are a little greater than zero at large  $m_*$ . It is because the small kaon mass decreases the contribution of the second term in the curly brace in Eq. (23). In Fig. 7 we show the results of  $D_{\text{rel}}$  for the  $K^+K^-$  BBC functions at  $T=160$  MeV. One can see that the differences between the relativistic and non-relativistic BBC functions become larger at the smaller temperature. The peak altitude of the BBC function is mainly determined by the particle distribution  $n_{\mathbf{k}_1, \mathbf{k}_2}$  [1, 2]. For fixed  $k$  the difference between the  $k^\mu u_\mu$  values in the relativistic and non-relativistic cases is enlarged in  $n_{\mathbf{k}_1, \mathbf{k}_2}$  at a small temperature [see Eq. (14)].

### 3 Summary and conclusion

We calculate the BBC functions of relativistic boson-antiboson pairs in high energy heavy ion collisions using the Monte Carlo method. The relativistic effects on the BBC functions of  $\phi\phi$  and  $K^+K^-$  pairs are investigated for different source velocities and pair momentum values. We find that the relativistic effect on the  $\phi\phi$  BBC functions at low pair momentum is small. However, at pair momentum  $k=0.8$  GeV/c and with zero source velocity, the effect may decrease the peak of BBC function by 30%. For a large source velocity, the non-relativistic BBC functions of  $\phi\phi$  appears as a slight distortion of lessening at small  $k$  values. Because kaon mass is smaller the relativistic effect on  $K^+K^-$  BBC function is more important than that on  $\phi\phi$  BBC function. For  $k=0.8$  GeV/c the maximum of the relative difference  $D_{\text{rel}}$  for the  $K^+K^-$  BBC functions at  $T=170$  MeV may reach 45%. On the other hand, we find that the difference

between the relativistic and non-relativistic BBC functions is sensitive to the particle freeze-out temperature. It becomes larger at a smaller freeze-out temperature. Further investigations of the BBC for hydrodynamical sources [9, 10] will be of interest.

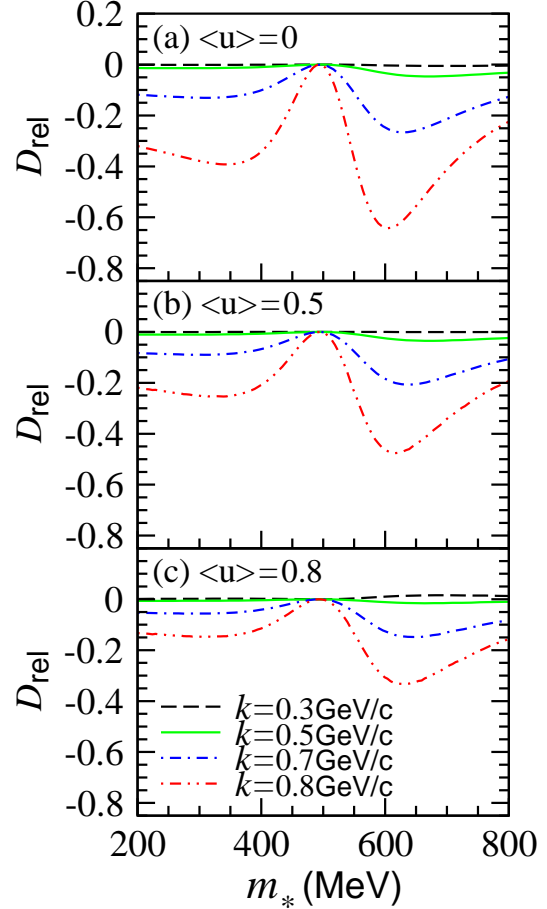


Fig. 7. The relative difference  $D_{\text{rel}}$  as a function of  $m_*$  for the  $K^+K^-$  BBC functions at  $T=160$  MeV and with different momentum  $k$  and  $\langle u \rangle$  values.

### References

- 1 M. Asakawa and T. Csörgő, Heavy Ion Physics **4** (1996) 233; hep-ph/9612331.
- 2 M. Asakawa, T. Csörgő and M. Gyulassy, Phys. Rev. Lett. **83**, (1999) 4013.
- 3 I. V. Andreev, M. Plümer and R. M. Weiner, Phys. Rev. Lett. **67** (1991) 3475.
- 4 M. Gyulassy, S. K. Kaufmann, and L. W. Wilson, Phys. Rev. C **20** (1979) 2267.
- 5 S. S. Padula, Y. Hama, G. Krein, P. K. Panda, T. Csörgő, Phys. Rev. C **73** (2006) 044906.
- 6 D. M. Dudek, S. S. Padula, Phys. Rev. C **82** (2010) 034905.
- 7 S. S. Padula, O. Socolowski, Jr., Phys. Rev. C **82** (2010) 034908.
- 8 Yu. M. Sinyukov, Nucl. Phys. **A566**, (1994) 589c.
- 9 M. J. Efaaf, Wei-Ning Zhang, M. Khaliliasr *et al.*, High Energy Phys. Nucl. Phys. **29** (2005) 46; *ibid.* 467.
- 10 M. J. Efaaf, Zhong-Qian Su, Wei-Ning Zhang, Chin. Phys. C **36** (2012) 410.